Laboratory calibration and characterization of video cameras

A. W. Burner, W. L. Snow, M. R. Shortis*, W. K. Goad

NASA Langley Research Center, Hampton, Virginia 23665, USA

*Department of Surveying and Land Information
The University of Melbourne, Parkville, Victoria 3052, Australia

ABSTRACT

Some techniques for laboratory calibration and characterization of video cameras used with frame grabber boards are presented. A laser-illuminated displaced reticle technique (with camera lens removed) is used to determine the camera/grabber effective horizontal and vertical pixel spacing as well as the angle of non-perpendicularity of the axes. The principal point of autocollimation and point of symmetry are found by illuminating the camera with an unexpanded laser beam, either aligned with the sensor or lens. Lens distortion and the principal distance are determined from images of a calibration plate suitably aligned with the camera. Calibration and characterization results for several video cameras are presented. Differences between these laboratory techniques and test range and plumb line calibration are noted.

1. INTRODUCTION

The calibration of close-range cameras is usually classified as either laboratory, on-the-job, or self-calibration[1]. Laboratory techniques all suffer the common disadvantage, compared to on-the-job or self-calibration, that the camera calibration is performed at a different time from when the photogrammetric measurement of interest is to be made. However, since on-the-job calibration or self-calibration is often not practical for near real-time video applications, the calibration of video cameras is generally restricted to laboratory methods. Goniometers and multicollimators are usually applied to cameras focused at infinity, whereas test ranges, the plumb line method, and the methods presented in this report have all been used successfully for the laboratory calibration of close-range video cameras.

The laboratory calibration techniques presented here were developed from earlier close-range photogrammetry with video tube cameras in which a reseau was placed on the tube faceplate to correct electronic distortion corrections and in which the plumb line method was used to determine the third order radial lens distortion[2]. This experience with a faceplate reseau led quite naturally to the use of a reticle with an array of dots photographically produced on film for use with solid-state sensors. The reticle (after measurement with a monocomparator) was placed on the protective coverglass of a solid-state sensor and illuminated with a collimated laser beam. The sensor/frame grabber parameters could then be determined from an affine transformation. The principal point of autocollimation and point of symmetry were found by illuminating the camera with an unexpanded laser beam, either aligned with the sensor or lens. The third order radial distortion was found by imaging an aligned target plate[3]. The purpose of this paper is to discuss further these techniques as well as to present a new laboratory technique to determine the principal distance.

2. SENSOR/FRAME GRABBER CALIBRATION

The sensor/frame grabber calibration is accomplished by comparing with an affine transformation a known image (in units of length) to the video image (in units of horizontal and vertical pixels). The photographically produced reticle mentioned above works well for cameras with good access to the sensor protective coverglass. However, some cameras require too much disassembly or the reticle cannot be placed near enough to the sensor surface due to IR blocking filters or external windows (for cooled sensors). In addition, movement of the film reticle to cover different areas of the sensor can be awkward and the vertical setup which is required for the film reticle is not convenient. For these reasons, the film reticle was replaced with a thin brass plate which has a 7 X 9 array of drilled holes 0.35 mm in diameter which slightly underfills the common 2/3 inch format sensor. The locations of the holes in the brass plate reticle were determined with an automatic monocomparator[4]. Measurements of the reticle were made at various orientations on the comparator traversing stage to test for differences in the horizontal and vertical scale and to average out possible small bias errors in the comparator. The uncertainty in the location of the holes is estimated to be ± 1 μm. The brass plate reticle can be used in a horizontal arrangement and displaced up to 50 mm from the sensor before the image spread due to diffraction causes interference between adjacent hole images. Such large displacements are not possible with a film reticle due to

distortions caused by film nonuniformity.

The experimental setup for the displaced reticle technique, shown in figure 1, consists of a collimated laser beam which illuminates the reticle. Also shown in figure 1 is a target plate used for measuring the principal distance and distortion once the sensor/grabber calibration is complete. The sensor/grabber calibration begins with only the camera (with lens removed) in place. The camera is mounted on rotation stages so that the unexpanded laser beam reflected from the sensor can be directed back onto the laser source to align the sensor to be perpendicular to the incident beam. There may be a number of reflections due to the diffraction grating-like nature of some sensors. The correct reflection to use is the one nearest the reflection from the protective coverglass which is identified by interference fringes caused by reflections from the front and back surfaces. The reticle is next positioned and adjusted to be perpendicular to the unexpanded laser beam with a front surface mirror placed in contact behind the reticle. Note that a reticle photographically produced on a plane parallel substrate of interferometric quality would have the advantage of a convenient reflecting surface for alignment of the reticle with the incident laser beam. For typical 2/3 inch format cameras the reticle is located about 25 mm from the sensor. Finally the collimating lens is positioned and aligned with the incident laser beam. The collimation is verified with a shearing plate interferometer.

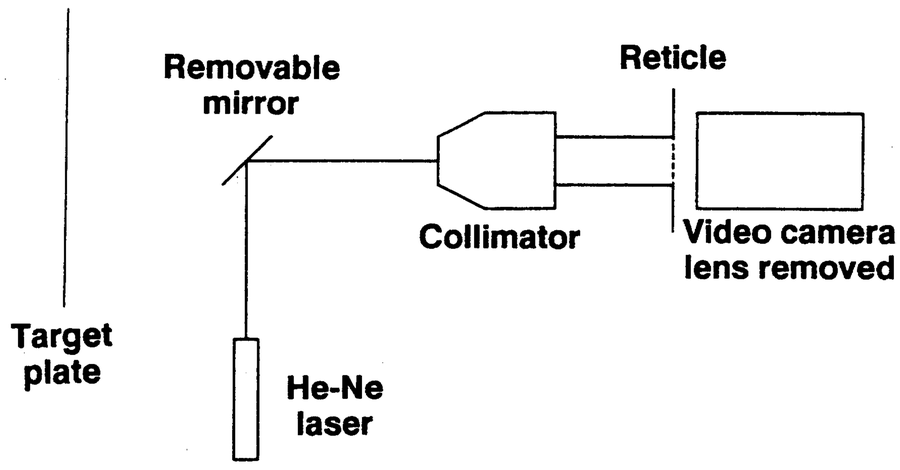

Figure 1. Laboratory calibration setup.

Interference fringes and diffraction noise are quite noticeable with the reticle removed due to the high coherence of the laser source. To reduce these effects, a reference image is taken without the reticle. The gray scale of an image taken with the reticle in place is then divided by the gray scale of the reference image before computing centroids. Such corrections for nonuniform illumination or varying pixel response are commonly made for astronomical images. Even though the nonuniformity of the illumination may appear rather severe, the effect on the sensor parameters is not great, since the centroiding errors vary on the image from hole to hole in a somewhat random manner. Note that the reference image can also serve as an aid in identifying and cleaning contamination on the protective coverglass or IR filter of the camera.

The gray level centroids of the diffraction spot from each hole of the reticle are computed after dividing by the reference image. As standard procedure, any background gray level is removed automatically by subtracting the maximum gray level on the perimeter of the area of interest for each centroid. The image formed in pixel coordinates x,y is then compared to the known reticle coordinates x',y' (in mm) with the following affine transformation

$$\begin{aligned} x' &= a_1 + a_2 x + a_3 y \\ y' &= b_1 + b_2 x + b_3 y \end{aligned} \tag{1}$$

The horizontal and vertical pixel spacings S_h,S_v and angle of non-perpendicularity of the pixel axes Φ are given by

$$\begin{aligned} S_h &= (a_2^{\,2} + b_2^{\,2})^{1/2} \\ S_v &= (a_3^{\,2} + b_3^{\,2})^{1/2} \\ \Phi &= \tan^{-1}(-b_2/a_2) - \tan^{-1}(a_3/b_3) \end{aligned} \tag{2}$$

The angle Φ is positive if the angle between the pixel axes is less than 90° . The transformation from pixel units to length (mm) units for an arbitrary video image is then given by the following equations (3). For Φ less than 0.1° , the approximations in equations (3) are valid to within 0.001 pixel for the common 2/3 inch format sensor.

$$\begin{aligned} x' &= S_h x + S_v y \sin\Phi \approx S_h x + S_v y \Phi \\ y' &= S_v y \cos\Phi \approx S_v y \end{aligned} \tag{3}$$

The displaced reticle technique is also useful for determining the variation in time (real or apparent) of the sensor parameters since a single frame of data is sufficient for computation. Confidence limits for variations in S_h are determined by apparent changes in S_v due to gray level centroiding variations in time. A possible repeatability test would consist of two steps. In step one, a single video frame is recorded with the reticle in place. The reticle is then removed

and a number of reference frames are recorded and used to compute the apparent variation in the sensor parameters due to any changes in time of the laser illumination. This determines the confidence limits for any variations found in step two. In step two, the reticle is replaced in the collimated beam and video frames of data are recorded over the time of interest to determine the parameter variations.

The displaced reticle technique can also be useful as a diagnostic tool for such things as determining the preferred method of synchronization, determining the effects of adding various video components or cabling, and determining differences in S_h due to different frame grabbers. For instance, to determine the difference in S_h when using a different frame grabber, the video signal (and sync or pixel clock if used) need only be switched from one grabber to the other and several video frames recorded with each grabber to determine apparent changes in S_h. These tests can be conducted and data reduced in just a few minutes.

3. LENS CALIBRATION

The lens calibration is carried out once the sensor parameters are determined. The principal point of autocollimation and the point of symmetry are first measured with a simple laser illumination technique. The principal distance and radial and decentering distortion coefficients are then determined with an approximately planar target field. The effects of different focus settings or the use of other lenses can be investigated without repeating the entire calibration since the sensor and lens calibrations are separate.

3.1 Principal point and point of symmetry

The principal point of autocollimation, usually denoted by x_p,y_p and simply called the principal point, is the foot of the perpendicular from the rear perspective center of the lens to the sensor surface. Distances on the image plane are measured from the principal point in the collinearity equations. The principal point for a solid-state camera can be found by aligning a low power laser beam with the normal to the sensor (with lens removed). The same setup as figure 1 with the collimator and reticle removed is used to make the measurement. With the lens mounted on the camera and approximately focused at infinity, the centroid of the focused laser spot on the video image locates the principal point. The laser beam need not pass exactly through the front perspective center of the lens, since for a reasonably corrected lens all parallel rays approximately intersect at the focal plane.

The point of symmetry for distortion, denoted here by x_o,y_o, can be thought of as the intersection of the optical axis of the lens with the sensor surface. Distances on the image plane are measured from this point for the computation of distortion. If the lens mount is parallel to the sensor, then the point of symmetry and principal point should coincide. If the lens mount is misaligned, then the point of symmetry and principal point no longer coincide and the angle of misalignment is the arctangent of the distance between the two points divided by the principal distance. Misalignment angles of up to 0.5° have been found for several solid-state cameras. The point of symmetry is found with the same setup as used for the principal point except that the low power laser beam is aligned with optical axis of the lens. Since the optical and mechanical axes of commercial grade lenses are typically equal to within 0.05° to 0.2°, and the mechanical axis is easier to determine, the laser beam is aligned with the mechanical axis. An unwedged mirror is placed either on the camera lens mount (with lens removed) or against the outer lens barrel and the laser beam aligned with the normal to the mirror. The centroid of the focused laser spot formed by the lens then locates the approximate point of symmetry, the approximation depending on how close the optical and mechanical axes coincide.

Neutral density filters, which are used to reduce the laser power density for these measurements, should have very little wedge (less than 0.01° total) so that the angle of the laser beam will not be changed appreciably when the filters are inserted in the beam after alignment. Variable density beamsplitters commonly used for holography have been found to be convenient for reducing the power density. To avoid the use of neutral density filters, a diffuse scatterer such as a piece of paper can be placed in the unexpanded laser beam near the laser which should be located many focal lengths from the camera. The unexpanded laser beam should pass through the center of the aperture stop if a diffuser is to be used.

3.2 Principal distance

The principal distance, often denoted by c and sometimes called the camera constant, is the perpendicular distance from the rear perspective center of the lens to the sensor plane. The determination of c is based upon the measurement of image scale over the central part of the image (near the point of symmetry and corrected for third order radial distortion)

as a function of the inverse of the object distance. The same focus setting of the lens is maintained throughout the measurement. The image scale is multiplied by the object distance at each new location of the camera to give c, which is plotted as a function of the inverse object distance. If the object distance is correctly measured from the front perspective center, then the measured values of c at each object distance should be equal (independent of object distance) and a slope of zero results. Any bias error in the object distance will cause the slope of the measured values of c versus inverse object distance to be nonzero. In the following it is shown that to a very good approximation the y-intercept of this nearly linear relationship is the true value of c.

Let c represent the true principal distance, which is independent of object distance, and c_m represent the measured value of c at object distance Z_m. The object distance Z_m is measured from some convenient point on the camera such as the front of the lens which is located an unknown distance b from the front perspective center. The true object distance Z (which should be correctly measured from the front perspective center) is then related to Z_m by $Z = Z_m - b$. The image scale M can be expressed as

$$M = c_m / Z_m = c / Z \tag{4}$$

Equation (4) is solved for c_m, and $(Z_m - b)$ substituted for Z, to give equation (5). The approximation is made because generally Z_m will be much greater than b.

$$c_m = c\, Z_m / Z = c\,(1 - b / Z_m)^{-1} \approx c + c\, b / Z_m \tag{5}$$

Thus c_m is approximately linear with $1/Z_m$ with a y-intercept equal to c. The distance b from the reference point on the lens to the front perspective center is found by dividing the slope by c. The measured object distance Z_m can then be corrected with this first estimate of b and c_m can be recomputed from the image scale and the new value of Z_m. Equation (5) can then be used to determine an improved estimate of c and b. After the second iteration, b should be nearly zero. The measured values of the principal distance c_m then become independent of the object distance and yield the true value of c. The standard deviation of the y-intercept (from the first order least squares solution of equation (5)) is used as an estimate of the error in c.

The target plate used for the distortion measurement is used as the object field in the determination of c. This 91 X 91 cm plate contains 323 white targets, each 6 mm in diameter, on a black background. The 3-D coordinates of the targets were measured with a large coordinate measuring machine to an estimated uncertainty of ±0.05 mm. For future work retroreflective targets can be used to reduce lighting variations across individual targets to lessen the effect on the measurements of the principal distance and distortion. Measurements from the 3-D coordinate measuring machine can be used as starting values and to establish scale for a multi-station single camera bundle adjustment. A large format film camera (CRC-1) can improve the precision of the targets. Note that only the central 9 targets surrounding the point of symmetry are used to determine image scale to reduce the dependence on possible lens distortion.

The measurement of c assumes that the camera image plane is parallel to the object field X,Y plane. The evenly spaced array of mounting holes and flat surface plate on a standard vibration isolation table are used as reference to align the target plate and camera, making use of the laser beam in the setup of figure 1 and a carpenter's square. Three targets on the perimeter of the plate are used to establish the X,Y plane for the target plate. The sensor is aligned parallel to the X,Y plane of the target plate in the same manner as for the measurement of x_p,y_p. The camera is positioned at a distance from the target plate such that the central 9 targets which surround the point of symmetry cover no more than 1/4 of the image field. Video images are recorded at a number of object distances as the camera is translated away from the target plate. A change in object distance of 1 - 2 m is desirable to improve the determination of the y-intercept and slope in the linear least squares solution. At each object distance the lens is removed, the camera is aligned with the laser beam, the lens is remounted using reference marks on the lens, and the object distance is measured. Thus alignment errors, errors due to variations in lens remounting, and the measurement error in Z_m are carried in the data set (as well as the basic bias error b) and contribute to the standard deviations of the linear least squares solution. These standard deviations are a reasonable estimate of the measurement error unlike a determination at a single object distance in which these errors produce a bias which does not contribute significantly to the standard deviation. The calculation of image scale and c_m are made at the same time as the distortion calculation as discussed next.

3.3 Distortion

Distortion measurements are made at several object distances where a large number of targets cover the image plane. At each object distance gray level centroids of the targets in the video image are computed. The pixel coordinates are

transformed to units of length (mm) with equations (3) based on sensor parameters found in the earlier sensor calibration. The object field coordinates of the target plate are scaled to the image plane based upon the measured object distance Z_m and initial estimate of c, the latter typically computed from the focal length. The scaled object field coordinates are next conformally transformed by least squares to the video image using the 9 targets which surround the point of symmetry. The 9 targets are corrected for third order radial distortion K_1 once a reliable estimate for K_1 is established. The initial estimate of c is multiplied by the scale computed from the conformal coefficients (which should be close to 1) to yield c_m for that object distance. The values of c_m and Z_m at various object distances are then used to compute the true principal distance c as described above.

Radial and decentering coefficients are found by minimizing image plane residuals with least squares using all the targets which are imaged. The distortion model can consist of up to 3 coefficients of radial distortion, K_1, K_2, and K_3, and can include 2 coefficients of decentering distortion, P_1 and P_2. When the residuals remaining after correction are shown to be due to the lens and not to the measurement technique, further corrections are possible. Repeat tests, in which the target plate or camera is moved (or rotated 90 or 180 degrees) so that a different set of targets covers the same field of view, are useful for determining the validity of the residuals.

4. ERROR CONSIDERATIONS

A measure of error for the laboratory techniques described above is the standard deviation of the least squares coefficients. However the standard deviation does not completely describe the error since a bias may not affect the least squares adjustment. For example, a scale error in the known reticle coordinates will cause a corresponding scale error in S_h and S_v (but not the ratio of S_h to S_v), but will not affect the standard deviations found from least squares. Also alignment error may go undetected in a single least squares adjustment. For this reason the error analysis should include not only the least squares estimates of the standard deviations of the coefficients, but also estimates based on potential bias error and variations due to repetitions in which the entire experimental procedure is repeated.

The least squares computation for a sensor/grabber calibration from a single video frame (and reference frame) yields standard deviation estimates for the affine coefficients which can be used in equations (2) to compute standard deviation estimates for S_h, S_v, and Φ. Typical values for short term (17 sec) and long term (1 hr) repeatability are compared to standard deviations computed from a single frame in Table 1. If the reference image is not used, the single frame standard deviations for S_h, S_v, and Φ increase to 0.0015 μm, 0.0023 μm, and 0.012° respectively. The least squares rms residuals for a single frame are typically around 1 μm (0.08 pixel). By moving the reticle to cover different parts of the sensor and comparing residuals, it was found that at least 0.6 μm (0.05 pixel) of the rms residuals is due to centroiding variations and may be a limit to the technique. The variation is due in part to incomplete correction for the nonuniform illumination and in part to variations which occur as the diffraction pattern from a hole covers different photodetection sites for repeat setups. The reticle can be rotated 90° and data taken to test for any scale differences in the axes of the assumed reticle coordinates. When the absolute sensor/grabber pixel spacings are of interest, the temperature of the reticle (which may rise 1° to 2° C when placed close to the camera) should be monitored and used to correct the reticle coordinates. Laser collimation can be checked by taking data at different distances from the camera.

ΔS_h (μm)	ΔS_v (μm)	$\Delta\Phi$ (deg)	
0.000098	0.00012	0.0036	25 repeats in 17 sec
0.00016	0.00025	0.0049	60 repeats in 1 hr
0.00069	0.0011	0.0058	single frame

Table 1. Comparison of repeatability and single frame error estimates.

The standard deviations for x_p,y_p from 10 measurements in which the entire alignment procedure is repeated to indicate the predicted variability for a single determination are 0.013 mm (1.1 pixel) and 0.0031 mm (0.23 pixel) respectively. Similar values are found for x_o,y_o. The larger deviation in x is presumably due to less rigid camera mounting in the horizontal plane. Note that typical centroid repeatabilities for a single setup when pixel clock locked are 0.005 pixel in x and y and that centroid repeatability alone is not a good indicator of the error in the principal point or point of symmetry. The point of symmetry suffers from an additional bias error in that the mechanical axis of the lens (which the laboratory technique is based upon) may not coincide with the optical axis. Typical misalignment angles of 0.05° to 0.2° would displace the apparent point of symmetry by 0.022 to 0.087 mm for a 25 mm focal length lens.

The standard deviation of c_m for a single frame is typically 0.008 mm as computed from the standard deviation of the scale (based on 9 targets). The standard deviation of unit weight for the transformation is typically around 1 μm. Note that the error in c_m at a single object distance may be much greater than the indicated 0.008 mm since Z_m may differ from the true object distance Z by unknown bias error b. With multiple frames (typically 9) of data at various object distances in a first order least squares solution, b can be found to 0.3 mm based upon the error in the slope, and the true principal distance c can be found to 0.005 mm based upon the error in the y-intercept. The principal distance depends on S_h and S_v since they determine the scale of the video image. Also note that lighting variations across individual targets on the target plate can cause error in the measurement of both principal distance and distortion. The computation of c is relatively insensitive to the value of radial distortion used initially because only the central 1/4 or less of the image plane is used for the transformation. Assuming the camera is translated from 1 to 2 m from the target plane for the determination of c, the error in the y-intercept is 0.006 mm for a 13 mm focal length video lens with a large value for K_1 (10^{-3} mm^{-2}) if the central 9 targets are not corrected. Since K_1 can typically be measured to better than 1 %, the effect of K_1 on the measurement of the principal distance can be neglected if the central 9 targets are corrected.

K_1	K_2	P_1	P_2
0.0068	0.052	0.28	0.10

Table 2. Fractional standard deviations for a single video frame.

The standard deviations as a fraction of the distortion coefficients for a 13 mm video lens are presented in Table 2. Note that variations in P_1 and P_2 between repeat setups can be several times larger than the standard deviations listed in Table 2. The distortion measurement is dependent on the sensor/grabber parameters and the initial estimate of K_1 used to correct the central 9 targets since they determine the image scale. The distortion measurement is independent of the principal distance and, if all the targets are in the XY plane, it is independent of the object distance. There is a slight dependence on the object distance as well as the location of the object plane origin for 3-D target fields. The values used for the point of symmetry also affect the distortion measurement. The effects of the various parameters mentioned above can be determined for a particular lens by substitution. For typical tolerances, the effect on the distortion coefficients is generally less than those of Table 2. However, decentering distortion is found to be very sensitive to the point of symmetry, with changes of over 200 % noted for an apparent displacement of x_o,y_o of only 0.1 mm.

ΔS_h (μm)	ΔS_v (μm)	Φ (deg)	
0.0008	0.0015	-0.001	CCDA1
-0.0013	-0.0015	0.011	CCDA2
0.0002	-0.0002	-0.010	CCDA3
0.0008	0.0008	0.010	CCDA4
0.0506	-0.0068	-0.008	CCDB1
0.0498	-0.0103	-0.009	CCDB2
0.0391	0.1585	0.114	CID1
0.0400	0.1516	0.119	CID2

Table 3. Differences from manufacturers' specifications.

5. CALIBRATION/CHARACTERIZATION EXAMPLES

Various laboratory techniques have been used at NASA Langley to calibrate and characterize video cameras for the past 5 years. Several high resolution tube cameras have been calibrated and, more recently, 8 solid-state cameras, including 6 CCD cameras from two different manufacturers and 2 CID cameras. Sensor/frame grabber calibration data for the 8 solid-state cameras are presented in Table 3 as differences from the manufacturers' specifications. The manufacturer's specification for S_h multiplied by the ratio of the nominal pixel clock frequencies of the camera and grabber was used as reference. For the CCD cameras operated in frame transfer mode, half of the vertical pixel dimension was used as reference because of the electronic shift of the photo-integration site in the vertical direction between video fields which yields an effective vertical pixel spacing of half of the pixel size on the chip. The measured sensor/grabber parameters for the CCD cameras from manufacturer A are equal to the specifications for the 4 cameras to within measurement error. However, the 2 CCD cameras from manufacturer B and the 2 CID cameras have significant differences in both S_h and S_v. The 2 CID cameras also have a significant angle of non-perpendicularity Φ.

The displaced reticle technique has been used to compare frame grabbers from the same manufacturer and also to compare sensor/grabber parameters for a single board operated in different computers. Differences in S_h up to 0.095 μm have been measured. Differences due to camera or grabber synchronization have also been determined. For instance, it was verified that to within experimental error a constant value for S_h was obtained independent of which computer the grabber resided, if the grabber is pixel clock locked to the camera. However, significant differences were noted for S_h when not pixel clock locked. It was also noted that time variations of S_h were 10 times as great when

operated without pixel clock lock. The displaced reticle technique has also been used to investigate centroid repeatability as a function of location on the video image which can occur when not pixel clock locked. In figure 2 the variation in the x direction in pixels is plotted versus time for 7 dots located near the start of video (left column) and for 7 dots located near the end of video (right column) with genlock on. The orientation of the 9 X 7 array of dots is shown at the bottom of the figure. Note the increased variation near the end of video (right column) and also that the variation is almost independent of video image height. This would imply that the entire image is expanding and contracting in time, with the start of video essentially fixed. Figure 2 points out the need to sometimes determine centroid repeatability as a function of location on the video image.

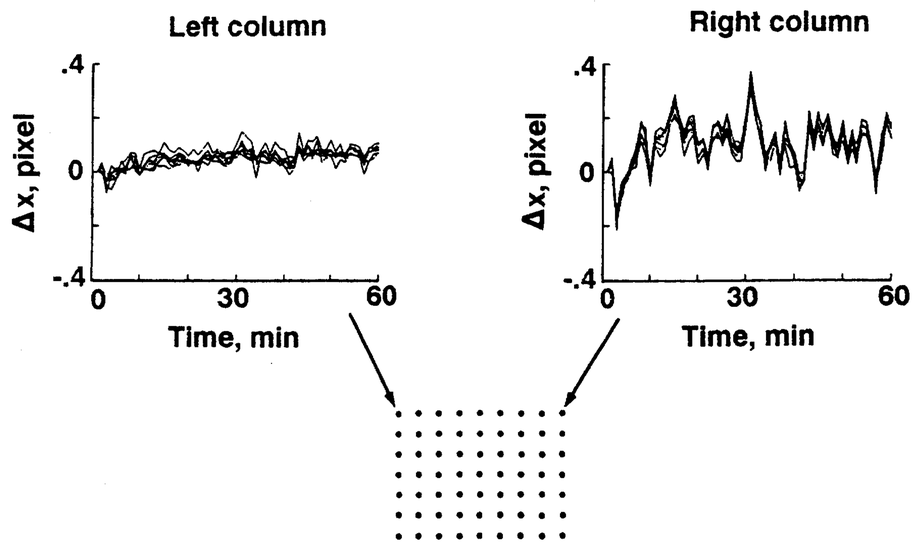

Figure 2. Centroid repeatability as a function of location on video image.

Determining calibration parameters individually, instead of simultaneously as in a photogrammetric calibration, can sometimes aid in deducing the cause of changes which may occur in video cameras. For instance, repeat measurements were made on a lens and camera for which earlier measurements of x_p,y_p and x_o,y_o were available. For this particular lens and camera, the first and second measurements differed by much more than the repeatability. It was discovered that a user of the camera between the first and second measurements had adjusted the back focus of the camera. The back focus adjustment for this camera consists of a slotted screw arrangement which holds the sensor mount to the camera case. The lens mount is rigidly attached to the camera case whereas the sensor mount is free to slide back and forth toward the lens mount to adjust the back focus. In such an arrangement, the angular alignment of the sensor to the lens can easily be altered during a back focus adjustment which would alter the values for x_p,y_p and x_o,y_o and account for the discrepancy between the first and second measurements. This discrepancy was noted and accounted for without solving for other lens parameters, whereas in a simultaneous solution the discrepancy may have been masked or muddled by the additional lens parameters.

The most significant distortion coefficient found for a number of video camera lenses has been negative third order radial K_1, or barrel distortion. Measured values for K_1, expressed as a percentage of maximum image height, range from 0.3 % for 25 and 50 mm focal length lenses to 3 % for 13 mm lenses. Note that a tolerance of 1 % is usually desired for imaging lenses. Residual distortion plots before and after correction for a 13 mm focal length video lens are shown in figure 3. The field of view contained 221 targets. Third and fifth order radial distortion K_1 and K_2 plus decentering distortion P_1 and P_2 were found to be significant and used to correct the data. Maximum residuals at the edge of field were reduced from 130 μm (10.4 pixel) to 7 μm (0.56 pixel) after correction. The standard deviation of unit weight for the distortion solution is 1.6 μm (0.13 pixel) when solving for radial and decentering distortion and 2.4 μm (0.19 pixel) when solving for K_1 alone.

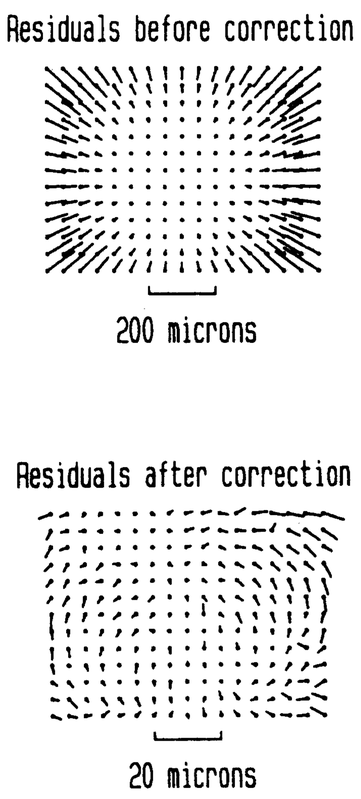

Figure 3. Residual distortion plots for a 13 mm lens before and after correction.

6. COMPARISON TO TEST RANGE AND PLUMB LINE CALIBRATION

During the past decade, the capabilities in analytical photogrammetry for industrial use have been expanded at NASA Langley due to the efforts of R. R. Adams and the acquisition of state-of-the-art large format film cameras, an automatic monocomparator, and user friendly software for data reduction[4]. Some examples of this work are presented in reference 5. Recently these capabilities have been further expanded to include video cameras as well with the development of analytical photogrammetric and plumb line code especially designed for video frame grabbers. This code was developed by one of the authors of this report (MRS) while a National Research Council Senior Research Associate at NASA Langley. A few of the operational differences between the laboratory techniques and test range and plumb line

calibration are discussed below.

Test range calibration has the advantage compared to the laboratory techniques described above that the photography can be more representative of operational conditions if the range is well designed and appropriate. A full set of calibration parameters can be derived with a reasonable degree of independence if the network is highly convergent, there is a large range of depth in the target and/or camera station array, and a variety of camera roll angles are used. However there are inevitable correlations between the internal camera calibration and the external orientation parameters, as well as correlations within each group, from the test range network. Correlations will be present even in a very well designed network which incorporates all available strategies to minimize correlations. Therefore the derived parameters are not likely to be accurately representative of their actual effects. In the laboratory techniques presented above, the interior calibration parameters are found essentially independently and separately and are only very weakly correlated with each other or exterior orientation parameters (due to misalignment).

One possibility to calibrate close-range video cameras is to use data from both plumb line and test range calibrations with the camera set at a fixed focus for a specific project. The plumb line calibration would supply accurate, independent lens distortion data, whilst the test range calibration would supply (correlated) parameters for the principal point location and principal distance, plus orthogonality and affinity of the sensor. Note that there is a strong analogy between plumb line calibration and the target plate technique described above, by virtue of the independence and accuracy of the distortion parameters in each case. One way to obtain the single camera, multi-station views necessary for calibration with a camera fixed in location is to rotate a small test range to various positions while keeping it in the field of view of the fixed camera. By mounting the camera on a stage which allows for rotation about the optical axis, the rolls necessary for calibration are possible. Several video cameras have been calibrated in this way with a plumb line calibration used to determine distortion. These tests emphasized to us the relative ease and speed of data acquisition possible when using analytical photogrammetry for video camera calibration. A complete set of 9 single camera multi-station views and plumb line data sufficient for calibration can be taken in several minutes, whereas a data set to determine distortion and the principal distance using the above laboratory techniques may take up to 1 hour to complete. This increased data recording time for the laboratory techniques is required for alignment and measurements which are time consuming (and can introduce additional error) and which are considered to be major disadvantages. Further comparison tests with test range and plumb line calibration are being conducted and are expected to be the subject of a future report.

7. CONCLUDING REMARKS

The laboratory techniques presented here are useful for calibrating close-range video cameras without the inherent correlation of interior calibration and exterior orientation parameters noted for test range calibration. These laboratory techniques are particularly suited to test for apparent changes in interior calibration parameters. Disadvantages of these techniques, compared to test range and plumb line calibrations, are that alignment and measurements are necessary which are time consuming (and can introduce additional error). It is not claimed here that these laboratory techniques are better or should be necessarily favored over other calibration techniques. They are simply, in some cases, different ways to achieve the same end result -- a suitably calibrated and characterized video camera.

8. REFERENCES

1. J. G. Fryer, "Camera Calibration In Non-Topographic Photogrammetry," Chapt. 5, Non-Topographic Photogrammetry, edited by H. M. Karara, 2nd ed., pp. 59-69, ASP&RS, Falls Church, 1989.
2. A. W. Burner, W. L. Snow, W. K. Goad , "Close-Range Photogrammetry with Video Cameras," 51st Annual Meeting ASP vol. 1, pp. 62-77, Mar. 1985.
3. A. W. Burner, W. L. Snow, W. K. Goad, B. A. Childers, "A Digital Video Model Deformation System," ICIASF '87 RECORD, IEEE, pp. 210-220, June 1987.
4. D. C. Brown, "AutoSet, an Automated Monocomparator Optimized for Industrial Photogrammetry," International Conference and Workshop on Analytical Instrumentation, Phoenix, AZ, Nov. 1987.
5. M. R. Shortis, "Industrial Photogrammetry at the NASA Langley Research Center," Symposium on Surveillance and Monitoring Surveys, University of Melbourne, Nov. 1989.